3.3 Wear Induced by Normal Compression

A stationary load such as a parked vehicle, the load from a storage bin, or even the heel of a standing pedestrian, will exert direct compression on the concrete surface. Even without the presence of lateral shear forces, this compression has the potential to abrade the surface. Wear induced by normal compression depends on the intensity of the compression, as well as the elasticity, hardness and toughness of the materials in contact.

There are three possible outcomes of surfaces making contact:

1. Adhesion
2. Deformation
3. Cracking

Figure 3.3 shows seven types of surface contact resulting from compression at asperities, each involving either adhesion, deformation or cracking. Deformation may either be ‘elastic’or ‘plastic’, while cracking may take the form of ‘cone’ cracks, ‘lateral’ cracks, or ‘axial’ cracks.

These various types of surface contact are discussed in greater detail in 3.3.1 through 3.3.7.

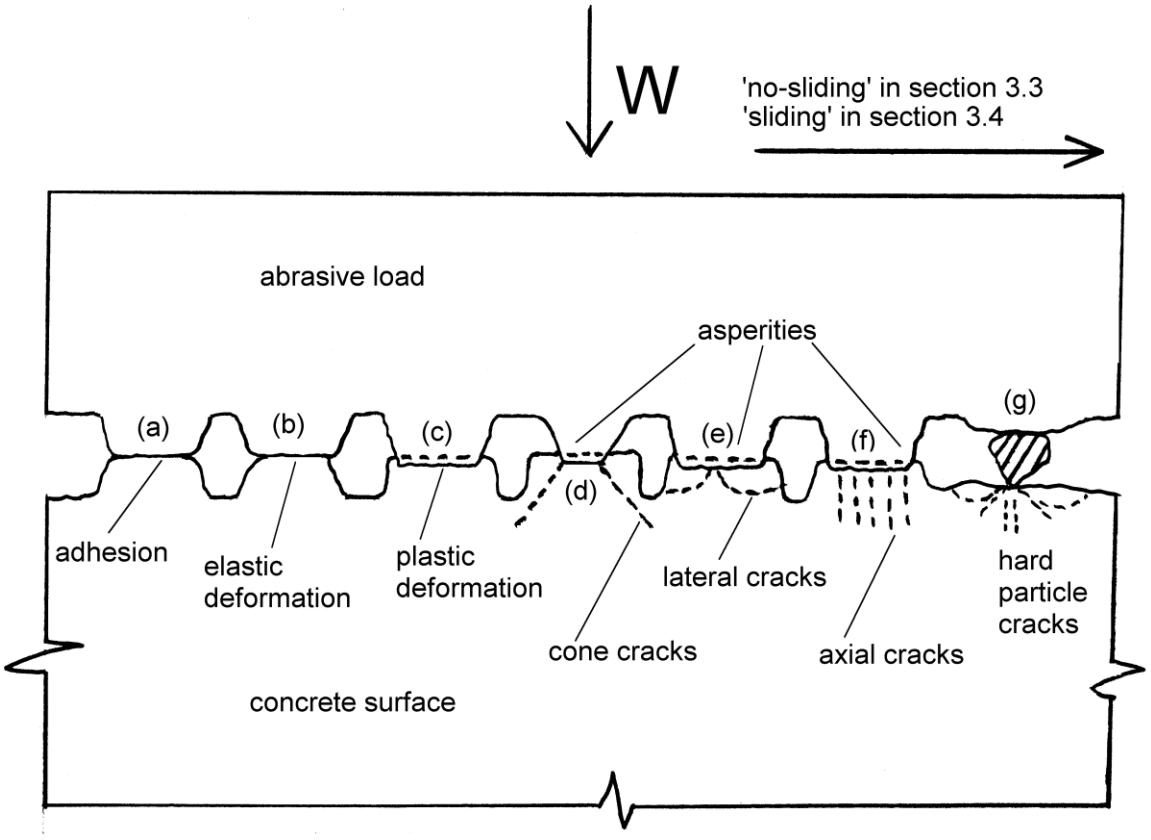

Figure 3.3 Model illustrating seven types of surface contact, resulting in either adhesion, deformation or cracking; (a) adhesion; (b) elastic deformation; (c) plastic deformation; (d) cone cracks; (e) lateral cracks; (f) axial cracks; (g) hard particle contact

3.3.1 Adhesion

Adhesion is the force of attraction between two surfaces in intimate contact as a result of attractions between their respective atoms or molecules. Compression between two surfaces brings the asperities of the surfaces into intimate contact, as shown in figure 3.3(a) and therefore is something of a 'catalyst' in the adhesion process.

The atomic bonds responsible for adhesion may be ionic (attraction of oppositely charged ions), covalent (where two atoms are associated by sharing their outer shell electrons), or metallic (where the outer shell electrons move throughout the crystal, attracted to the +ve cores of all the cations, so holding the crystal together). For example the strong adhesive forces operating between certain metals across asperity junctions is the result of metallic bonding between the respective atoms of the two metals.

Intermolecular bonds, on the other hand, known as van der Waal's forces, are much weaker than atomic bonds.

Adhesion, is really only of any consequence in metals where the two surfaces in contact are very smooth, ductile, and atomically clean. For example if the rounded end of a brass or steel rod is degreased and abraded to remove some of the surface contamination (e.g. oxides), and then pressed onto the freshly scraped surface of a block of indium, strong adhesion will occur, requiring appreciable force to detach the rod. On inspection separated fragments of indium are seen to adhere to the rod, showing that the adhesive forces at the interface are stronger than the cohesive strength of the indium itself. This amounts to adhesive wear.

However, all metals other than gold oxidise to some extent, and this layer of oxidised material very substantially reduces adhesive attraction. Gaseous films of oxygen and water vapour further undermine intimate contact and so the potential for adhesive wear.

Adhesive forces (of covalent, ionic or van der Waals origin) are also present between certain brittle materials in contact, but are not nearly as significant as in clean metals in the absence of oxygen. (Hutchings(1992) reports on adhesive forces in ceramics). It is probable that some covalent bonds will develop between concrete and an abrasive particle that is calcareous or siliceous in nature. An example may be a loose aggregate particle lying on a concrete surface that is compressed by a truck tyre. The high stress exerted by the aggregate particle upon the concrete surface will doubtless cause some crushing of asperities on both the aggregate particle and the concrete surface. It is therefore conceivable that the two surfaces make atomically clean contact at the points where asperity crushing has occurred, and some transfer of material by adhesion may occur. However, the brittle material will also deform elastically in other regions where a less severe form of contact is made. The elastic strain energy in these regions, associated with elastic deformation, will generally exceed whatever adhesive forces may occur at other asperities, so that on unloading the adhesive bonds are broken, and the surfaces are not held together. To what extent material is transferred (possibly on an atomic scale) from one surface to another when asperity contact is broken is not known. To the author's knowledge, no attempt has ever been made to quantify such adhesion wear effects in concrete.

3.3.2 Elastic Deformation

The degree of damage/wear that stationary loads inflict on concrete surfaces depends on how concentrated the load is, and this is normally understood as force divided by the apparent area of contact. More important however is the pressure experienced at the many individual microscopic asperities. Clearly very smooth surfaces in contact will have vastly more contact points to distribute the load than relatively rough surfaces, so that the level of stress in the former may remain in the elastic realm while that of the latter will be sufficiently high to cause plastic deformation or crushing.

3.3.2.1 Smooth-Surface Contact

If both surfaces are sufficiently smooth and aligned, there will be so many contact points that the concrete asperities will respond elastically to the applied compression. This means that the strain goes out of the asperities immediately the load is removed, with no damage to the asperities and consequent loss of material i.e. wear (ignoring any possible adhesion here).

Figure 3.4 illustrates a ‘smooth-surface contact’. The concrete is idealistically considered to be perfectly smooth, while the applied load is shown to have many asperities, considered in this example to be spherical shaped at their points of contact, and all making equal contact with the concrete. In the initial stages of applying the load, its asperities deform the softer concrete elastically.

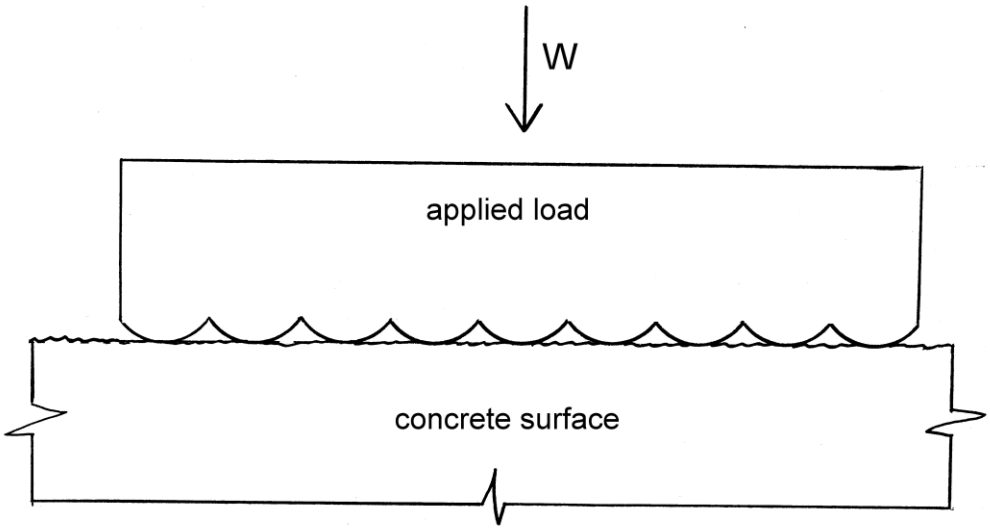

Figure 3.4 Microscopic presentation of contact between an array of hard and even protuberances pressing down on an idealistically smooth surface, resulting in elastic compression. The protuberances may for example model the asperities of a polished surface.

(This situation may also be reversed, i.e. the concrete protrusions may be larger relative to those of the load, particularly if the applied load is a smooth surface like a ball bearing, or a polished steel pad. The resulting effect, given further on in equations, 3.1 through 3.4 will nevertheless still be the same).

3.3.2.2 Blunt-Object Contact

Figure 3.3 (b) represents a single asperity of the load making contact with a single 'blunt' asperity of the counterface. If this asperity is considered to be spherical at its tip, then it will resemble figure 3.5, or one of the asperities of figure 3.4.

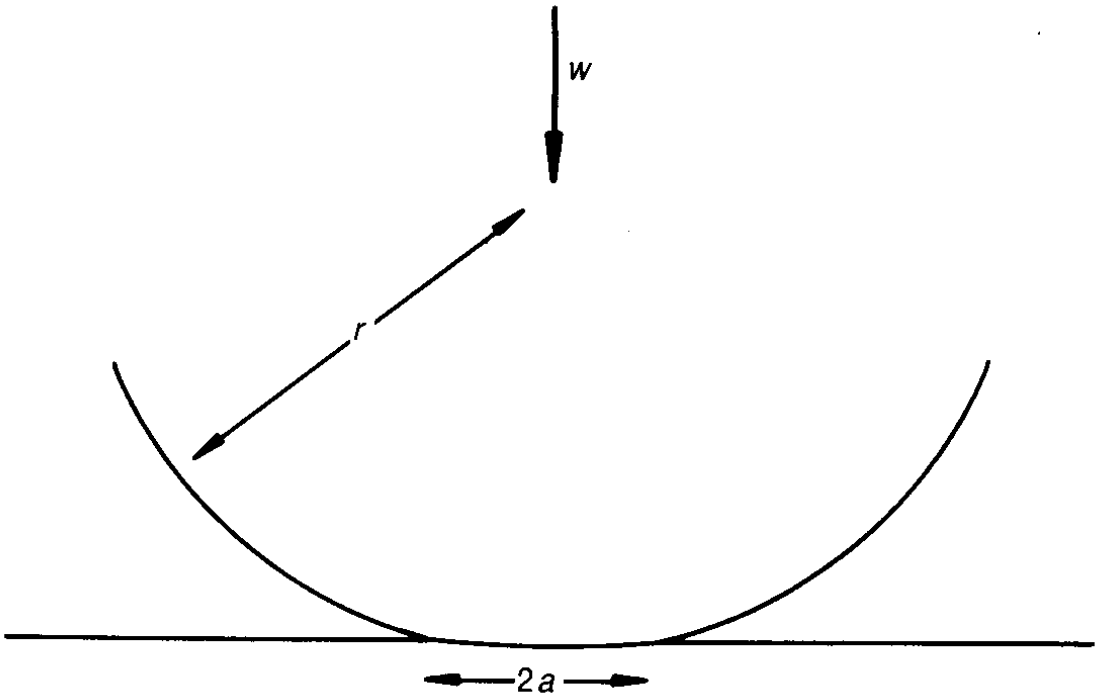

Figure 3.5 Contact between a hard smooth spherical load pressing down on an idealistically smooth concrete surface. [Hutchings(1992), pg15].

Hertz showed that for a hard spherical indenter penetrating a softer counterface, both materials acting elastically, the radius of the contact circle of figure 3.5 is given by:

$a = (3Wr/4E)^{1/3}$ …….(3.1)

where:

w = the load on an individual asperity
r = radius of the asperity
E = and average elastic modulus given by the expression:

$1/E = (1 - \gamma_1^2)/E_1 + (1 - \gamma_2^2)/E_2$ …….(3.2)

where E_1 and E_2, γ_1 and γ_2 represent the elastic moduli and Poison's ratios of the two respective surfaces.

It follows that the mean contact pressure is given by:

$p_{mean} = w/\pi a^2$ ……. (3.3)

The maximum pressure is given by:

$p_{max} = 3/2 \times p_{mean}$ ……. (3.4)

The pressure distribution in the material beneath the hard sphere is indicated in figure 3.6.

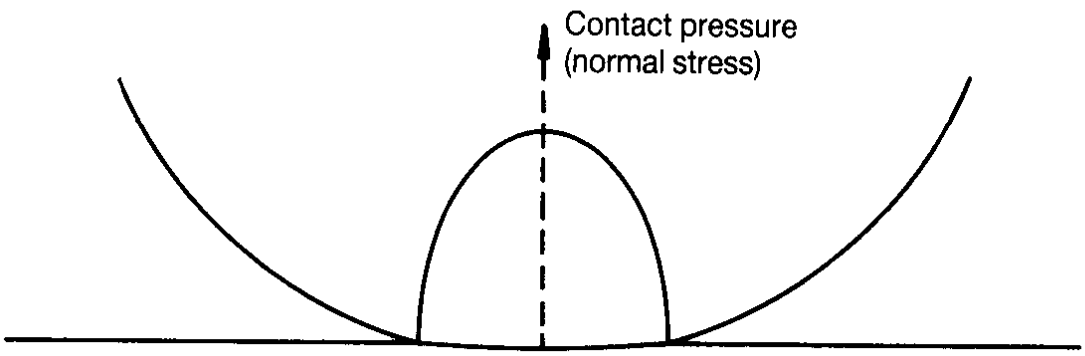

Figure 3.6 The distribution of normal stress (contact pressure) under a sphere loaded elastically against a plane. [Hutchings(1992), pg15].

Greenwood and Williamson applied Hertz's model for a surface where the asperities have a statistical distribution in terms of height, shape, and spacing, and found that:

$W = 4/3N.E.r^{1/2}\int_{d}^{\infty} y(z-d)^{3/2}.\phi(z)dz$ ……. (3.5)

Where:

N = the number of asperities that support the total load W (i.e. W = N.w)
y = height of the profile of the surface above a reference plane
z = the initial height of the asperities above the reference plane prior to compression
d = the height of the asperities above the reference plane after compression
r and E are the same as in equations (3.1) and (3.2)

Note that z-d therefore represents the shortening of the asperities associated with the elastic compression

$\int_{d}^{\infty}\phi(z)dz$ is the probability of z>d

Sectional conclusion: Mathematical models (expressions 3.1 through 3.5) have been developed that relate the applied load to the local geometry and the elastic moduli of the materials. It may be said that elastic deformation occurs where the compression in opposing asperities does not exceed the elastic limit of either surface. Elastic deformation 'disappears' on unloading, the material resuming its original form. Elastic deformation is therefore not associated with loss of material. Were it not for this concrete roads and floors would soon abrade away. But the relatively soft contact between a rubber tyre or leather sole ensures that these mechanisms apply in the majority of contacts.

3.3.3 Plastic Deformation

A metal or other surface that is coarsely ground rather than polished will have higher, fewer, and asperities that are less even, and the load is therefore substantially increased at the contact points. Therefore the probability of a given load resulting in plastic deformation is substantially increased, and in figure 3.3(c) the asperity of the hard load is shown to have depressed/deformed (in a platic sense) the oppossing asperity of the softer counterface.

In metals, once the yield criterion, Y, is satisfied, plastic flow begins at a depth of 0,47a beneath the surface of a hard spherical indenter of radius r (the indenter, at its tip, may be considered to have a configuration similar to figure 3.5). With further increase in load the zone of plastic deformation eventually reaches the surface. At this stage the radius 'a' is still less than r/100, and the load W has increased by a factor of 50 to 100 relative to the load corresponding to the beginning of plastic flow. The mean pressure, $p_{mean} = 3Y$. With further increases in load, there is a substantial flow of material while p_{mean} remains constant, so that the area becomes directly proportional to W.

Even in a brittle heterogeneous material such as concrete, it is probable that a degree of *plastic* behaviour takes place after the concrete ceases to behave in a fully elastic sense, and *before* brittle fracture in the form of the Hertzian cone cacks (see later in fig 3.8) occurs. This can be expected in the immediate vicinity of the concentrated load. 'Densification' rather than plasticity probably more aptly describes this post yield behaviour in concrete, the high compressive stresses resulting in localised microscopic crushing and consolidation, as pore cavities and microscopic air voids are closed up.

According to Hutchings(1992) the proportion of asperity contacts in a material under load at which plastic flow has occurred depends on the value of the plasticity index, ψ, where:

$$\psi = E/H(\sigma^*/r)^{1/2} \quad \ldots\ldots. \quad (3.6)$$

where:

r and E are as per equations (3.1) and (3.2). Note that E is related to the modulus of both surfaces.
H = the indentation hardness of the surface ($\approx 3Y$)
σ^* = the standard deviation of the distribution of the asperity heights

The quantity $(\sigma^*/r)^{1/2}$ is approximately equal to the average slope of the asperities, and it will be shown that this explains why very smooth surfaces behave more elastically than do rough surfaces.

Equation 3.6 is indeed very useful in predicting a surfaces's response to stress. A material with a low plasticity index implies predominantly elastic deformation, and conversely a high plasticity index implies that plastic deformation dominates. From expression (3.6) it is evident that a high plasticity index follows when the ratios E/H and $(\sigma^*/r)^{1/2}$ are relatively high. This expression explains why mild steel behaves more plastically than a cold worked steel. Both have the same elastic modulus, but mild steel has a much lower indentation hardness and hence higher E/H ratio.

Furthermore the expression $(\sigma^*/r)^{1/2}$, which approximately represents the average slope of the hills and valleys of the surfaces's asperities, explains why the surface of a machined plate, with characteristic deep and closely spaced grooves, will deform plastically under a given load relative to a polished surface. (The polished plate has many more contact points to sustain the load, thus retaining elastic behaviour. The surface of the applied load is assumed to be conformal, hard and smooth for both cases).

The effect of roughness on the plasticity index is shown in figure 3.7.

However, concrete only has limited plastic behaviour, which should in any event be understood predominantly as irreversable denisificaton.

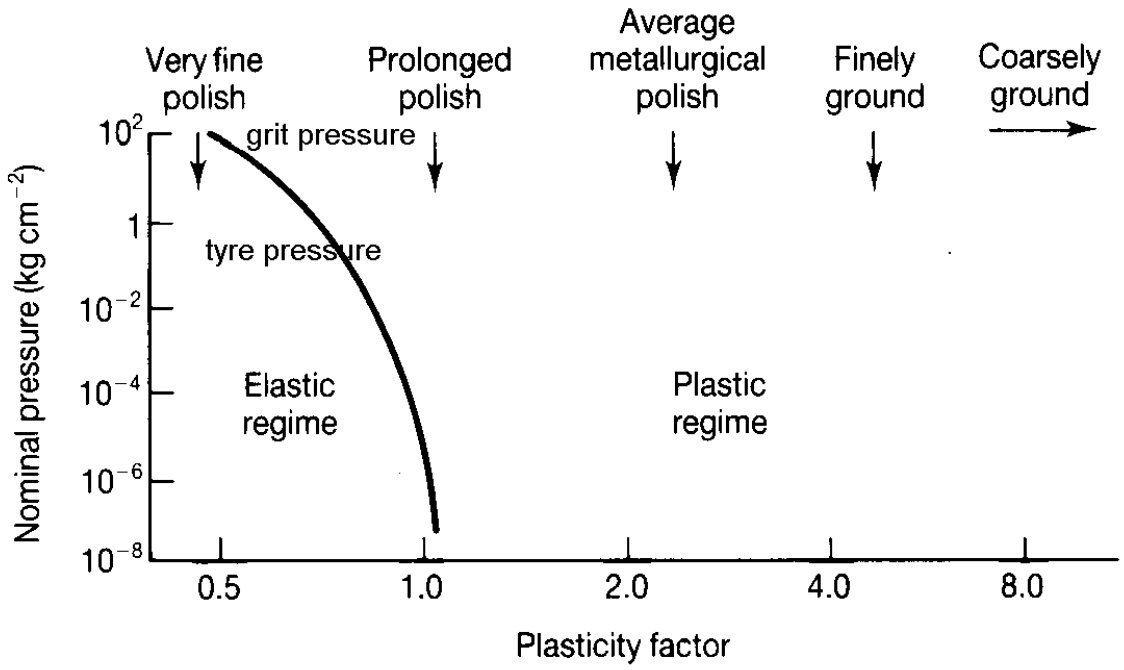

Figure 3.7 The effect of surface-roughness (as reflected by the plasticity index ψ) on the mode of deformation of asperities (plastic or elastic), for aluminium surfaces. [Hutchings(1992), pg20, from Tabor D, Friction, lubrication and wear, in Matijevic E (Ed), *Surface and Colloid Science* vol. 5, John Willey, 1972, pp 245-312]. Note that since all these surfaces are made of aluminium E/H is constant.

Concrete is known to have a much lower elastic modulus than steel, generally varying from a tenth to a quarter, depending mainly on compressive strength and aggregate selection. On the other hand H in concrete may be comparable or even superior to that of steel. [Hutchings(1992) shows that the indentation hardness of quartz, a common aggregate in concrete, ranges between 750 –1200 HV, which compares very favourably with that of Ferrite (α-Fe), ranging between 70 – 200, and that of chromium, ranging between 100 – 170 and that of tungsten, ranging between 260 – 1000]. Therefore in the expression E/H a lower numerator and equivalent or even higher denominator means that this ratio is much lower for concrete, and the material will therefore have a low plasticity index, especially in its elastic phase. However, in order for it to respond elastically, both the surface of the applied load and that of the concrete (counterface) will need to be very smooth as in 'very fine polish' in figure 3.7. Alternatively, the applied load should be very conformal (have the same shape of the counterface) as in rubber or leather.

Figure 3.7 also predicts that for a given value Ψ, there is a shift from an elastic response to a plastic behaviour as the load increases. On the other hand metals mostly deform plastically. They behave elastically at their asperities only if the surfaces are very smooth, conformal, and lightly loaded.

Figure 3.7 shows that the proportion of the asperity contacts that become plastic is determined both by the value of the plasticity index and the nominal pressure, but in

practice the plasticity index is far more important than the applied load, and dominates the behaviour.

To conclude it may be said that plastic deformation occurs where the level of compression exceeds the elastic limit of the material in question, causing yield or plastic flow. Characteristically metals deform plastically at their asperities, whereas in brittle materials ‘plastic’ behaviour may be synonymous with ‘densification’. The plasticity index is a very good indicator of whether a material will respond elastically or plastically, with plastic behavior favored in relatively rough surfaces with a high E and low H, and subject to higher loads. The effects of plastic deformation are permanent. Particularly in metals plastic deformation eventually leads to work hardening, loss in ductility, and fatigue. This results in some loss of asperity material.

Transition from Elastic/plastic deformation to Brittle Fracture

The foregoing discussions have shown that brittle materials, if sufficiently lightly and conformally loaded will deform elastically, with negligible wear. As the load increases a degree of plastic deformation/densification occurs.

However, in concrete, as load and stress increase, brittle fracture follows soon after the onset of plastic deformation. This is the most severe mode of abrasion wear.

In non-homogeneous ceramics the early stages of wear may be identified by cracks along grain boundaries leading to the loss of individual grains. However with increasing load, wear is identified with inter-granular fracture or even trans-granular fracture.

These mechanisms may also be identified in concrete/mortar. In this instance the aggregate/paste transition zone is known to be the weakest link (see section 2.5 for a fuller discussion on the transition zone). Cracks in this area are likely to lead to the loss of aggregate particles. With increasing load, inter-granular fractures and finally trans-granular fractures can also be expected.

Cracking is thus the third possible outcome of contact between surfaces, and generally occurs in brittle materials when subjected to a concentrated force.

Three types of cracks are considered below; cone cracks: lateral cracks; and axial cracks. With all three of these cracking mechanisms, cracks will initiate in the transition zone, progress to inter-granular and finally transgranular cracks may be expected. These concepts are explained in geater detail in 3.3.6.4.

3.3.4 Cone cracks

Hertzian cone cracks come about as a result of a hard but relatively blunt object pressing upon the surface of a brittle material. This is identified in figure 3.3 (d) on a microscopic/asperity scale. As the load increases, the material responds elastically, while a tensile stress, σ, develops in a direction normal to an inverted truncated cone (see figure 3.8), starting where the hard object comes out of the surface, (see fig 3.8). At a critical point, the material can no longer sustain any further increase in load. This corresponds to the maximum tensile stress $\sigma_{r\,max}$ acting at the edge of the circle of contact, at which point the concrete develops a classical Hertzian cone crack, with:

$\sigma_{r\,max} = (1 - 2\gamma) \cdot p_{mean}$ ……. (3.7)

where

γ = Poison's ratio of the counterface, and

$p_{mean} = w/(\pi a^2)$, as in equation 3.3

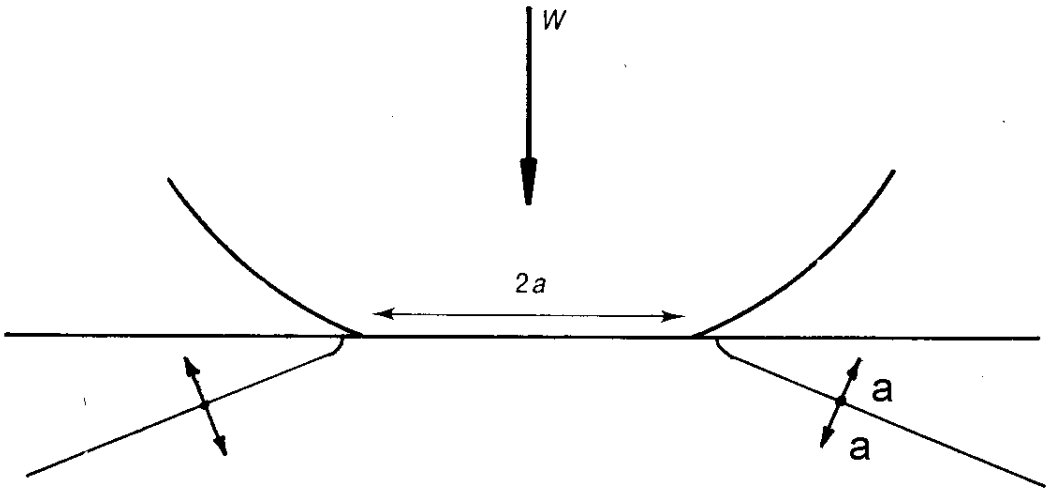

Figure 3.8 Microscopic presentation of contact between a hard smooth steel ball pressing down on an idealistically smooth concrete surface such that a Hertzian cone crack is generated. [Hutchings(1992), pg117].

This crack is generally not associated with wear. However should the load be removed and re-applied in the near vicinity, adjacent cone cracks may intersect, with the potential for loss of material.

In figure 3.3(d) Hertzian cone cracks are identified on a microscopic/asperity scale.

3.3.5 Lateral cracks

A very concentrated load such as may be applied by a sharp hard particle pressing down onto the surface of a predominantly brittle material results almost immediately in some plastic densification at the point of application followed by brittle fracture in the form of vertical and horizontal cracks. This process is fully illustrated in figure 3.9. The material affected by the lateral cracks is effectively severed beneath the surface [see figure 3.9(f)] and will easily be removed by subsequent abrasive actions such as scratching/scraping/rubbing.

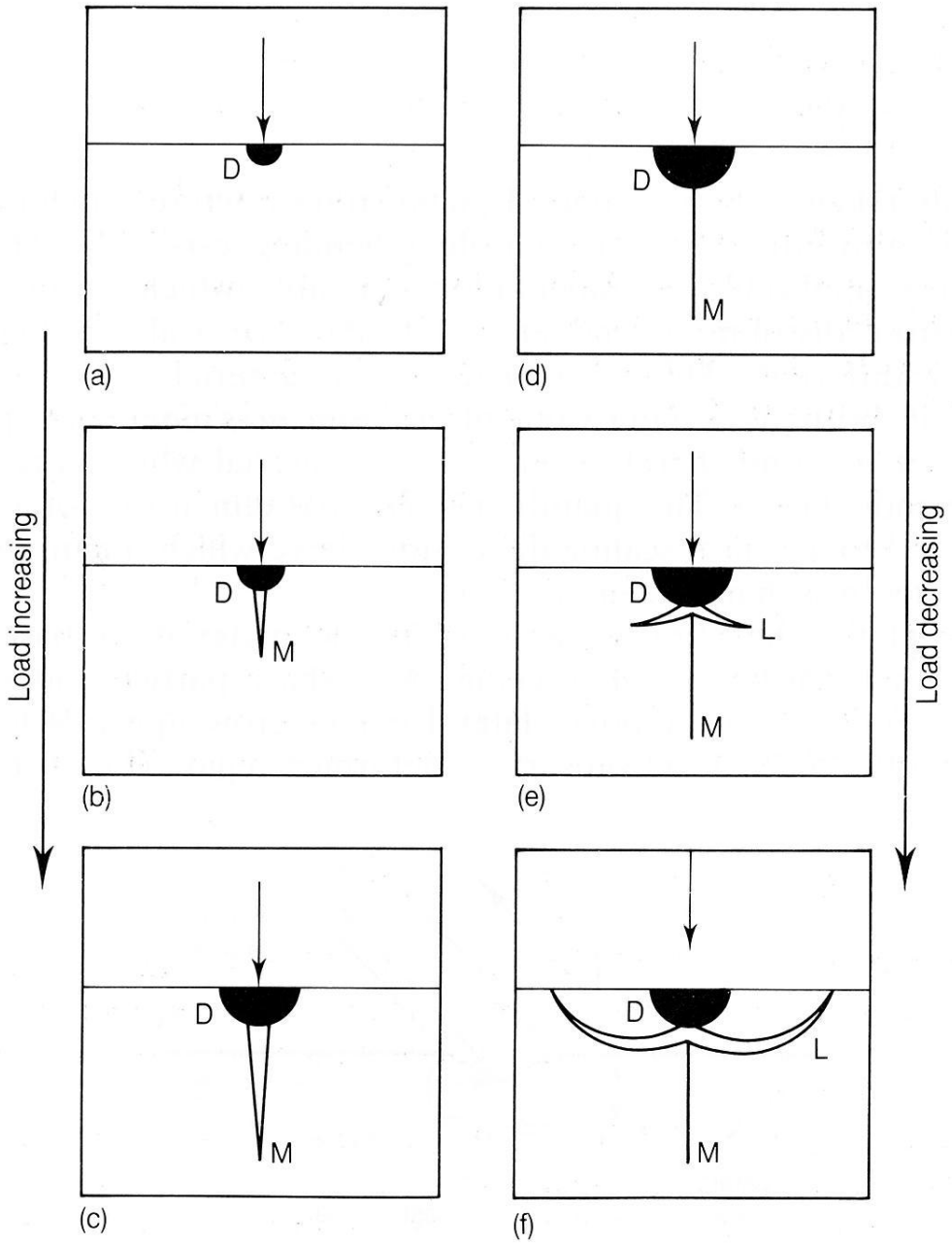

Figure 3.9 Crack formation in a brittle material due to indentation with a sharp point. The normal load increases from (a) to (c), and then is progressively reduced from (d) to (f). [Hutchings(1992), pg 151, from Lawn B R and Swain M V, J. Mat. Sci. 10, 113-122, 1975].

The point load in figure 3.9 could be a hard angular grit particle beneath a car tyre or pedestrians shoe.

Figure 3.9 (a) indicates that the intense stresses (shear and hydrostatic compression) are relieved by local plastic deformation/densification, at the point of contact.

Figure 3.9 (b) shows that as the load increases to a critical value, tensile stresses across the vertical mid-plane initiate a median vent crack.

Figure 3.9 (c) indicates the lengthening and widening of the median crack with further increasing load. The zone of plastic deformation/densification has also grown.

Figure 3.9 (d) shows that as unloading begins, the median crack closes, and is then stable, not extending further, and not associated with loss of material.

Figure 3.9 (e) shows that further unloading results in the formation of lateral vent cracks, driven by residual elastic stresses, caused by the relaxation of the deformed material around the region of contact.

Figure 3.9 (f) shows that as unloading is completed, the lateral cracks curve upwards, terminating at the free surface. It is these lateral cracks that are associated with loss of material when subjected to scratching/scraping/rubbing effects.

Brittle materials subject to concentrated loads develop the kind of lateral cracks described above when the load exceeds a critical value, w*. The value of w* depends on the fracture toughness of the material, Kc, and on its hardness. According to one theory:

$w^* \propto (K_c/H)^3.K_c$ ……. (3.8)

K_c is usually taken to be the mode I plane strain fracture toughness as measured in a bending test.

Given the exponential terms in this relationship it is clear that the resistance to fracture is greatly improved when Kc is increased and conversely greatly reduced when hardness is increased. (This principle was illustrated in figure 3.2).

It may be concluded that a hard sharp object pressed down upon a brittle surface results in lateral cracks beneath the surface. The material above the lateral cracks is effectively severed, resulting in measurable wear. Some hardness should be sacrificed for toughness in brittle materials subject to such loads.

Finally it is also conceivable that lateral cracks may originate from a relatively pointed microscopic asperity, since in this case the applied load makes contact with a very confined area, even if the load it is relatively flat. This is illustrated in figure 3.3(e).

3.3.6 Axial cracks

3.3.6.1 Introduction

Various outcomes of surfaces in contact have been discussed above (3.3.1 through 3.3.5), including two types of cracking (3.3.4 and 3.3.5). The focus of the studies was confined almost entirely to surface abrasion wear, which is very relevant, but the work was done on metallic and ceramic materials. This means that some interpretation is required before applying the findings to concrete surfaces. While some of the principles governing abrasion resistance and wear will be universal, others are not applicable.

By way of contrast the theory put forward below is based entirely on the testing of concrete, which is a most satisfactory position, but on the other hand the tests were made using standard concrete specimens subjected to standard compression and tensile tests, so that the findings apply to the bulk rather than surface characteristics of concrete. Nevertheless, it may be argued that a relatively tall and slender asperity in compression may experience the same mode of failure, on a microscopic scale, as a concrete cube or a cylinder that is crushed, particularly if the asperity has a similar aspect ratio. It is also conceivable that localised axial cracks may extend deeper into the concrete, to the sub-asperity zone, in the case of severe compression, such as may occur when a heavily loaded small steel wheel traverses the surface.

The term '*axial cracking'* is used here to describe cracks that propogate in the direction of the applied load. This consititutes another way that brittle surfaces can crack when subjected to high compressive stresses.

In other words there may be instances where mechanisms pertaining to abrasion are similar to those causing failure in compression or tension specimens. Assuming this is so, then much can be learned from the experimental work done on concrete cylinders, described by Newman(1997a). Some of these findings are reported in section 3.3.6.2 through 3.3.6.5

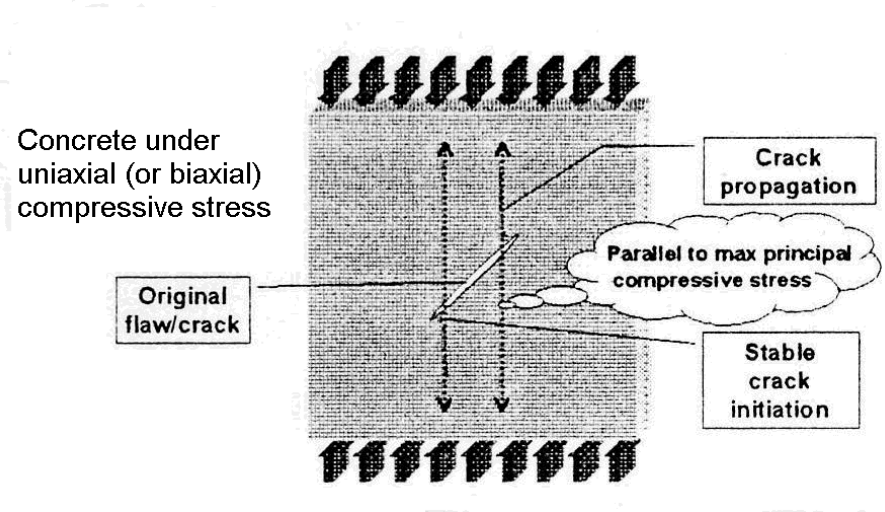

Figure 3.10 Fracture model for concrete, [Newman(1997a), pg 4].

Axial cracks are illustrated in figure 3.3 (f) on a microscopic/asperity scale, while macroscopically the cracks would resemble figure 3.11.

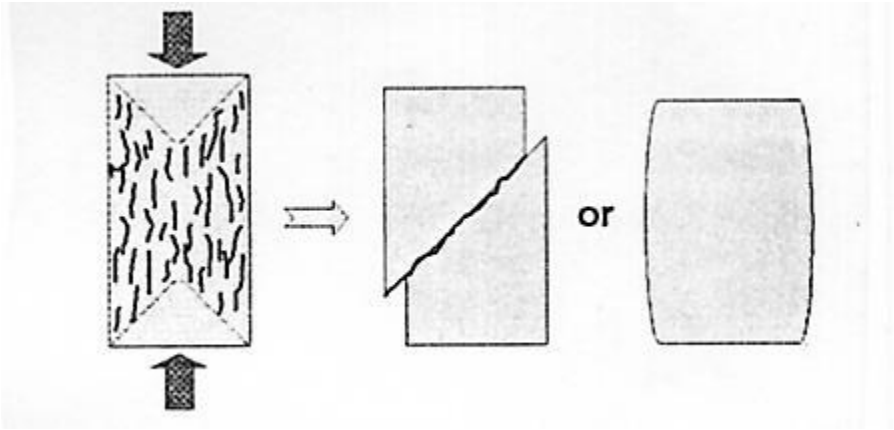

Figure 3.11 Failure modes in uniaxial compression, [Newman(1997a), pg 8].

Axial cracking begins with crack initiation, followed by crack propagation in line with the direction of the load, as indicated in figure 3.10. The cracks are initially stable, but continue to grow as the load is increased, in line with the direction of the load, eventually becoming self propagating and unstable at constant or even reducing load, leading to failure by shear or dilation as shown in figure 3.11. The process is described in greater detail below because the writer is of the opinion that it contributes significantly to compression related abrasion wear, and a better understanding of the mechanisms of 'axial cracking' will be helpful.

3.3.6.2 Crack Initiation and Fracture

Concrete cubes and cylinders subject to any state of stress can support loads of up to 40 to 60 percent of ultimate without any apparent signs of distress, although the stress strain relationship is not strictly linear and not completely reversible. As the load continues to be increased, soft but distinct noises of internal disruption can he heard until, at about 70 to 90 percent of ultimate, small fissures or cracks appear on the exterior (figure 3.11). These cracks spread and interconnect until, at ultimate load, the specimens are usually completely disrupted and fractured into a large number of pieces. The formation and propagation of small microscopic cracks, or microcracks (2 – 5 μm), have long been recognized as the causes of fracture and failure of concrete and the reason for the marked non-linearity of the stress-strain curve near ultimate (see figure 3.12).

3.3.6.3 Measurements of Crack Initiation and Propagation

The initiation and proliferation of microcracks produce irrecoverable changes in the internal structure of concrete, including the formation of voids and the dissipation of energy in the form of heat, mechanical vibrations and in the creation of new surfaces.

Various methods have been used to detect the structural changes accompanying crack formation and propagation, including; microscopic and X ray examination of the surface of specimens during loading and of sections cut from specimens after loading; photo-elastic coating; Moire interferometry; strain gauge and deflection readings during loading; measurements of ultrasonic pulse velocity through specimens under load; measurements of acoustic emissions and absorption of acoustic energy; and measurements of electrical resistivity changes of saturated specimens under load.

3.3.6.4 The Stages of Cracking in Concrete

The methods stated above have confirmed the progressive process of crack initiation, multiplication and stable propagation, through to ultimate disruption and failure following unstable crack propagation. These three stages are discussed below and illustrated in

figure 3.12.

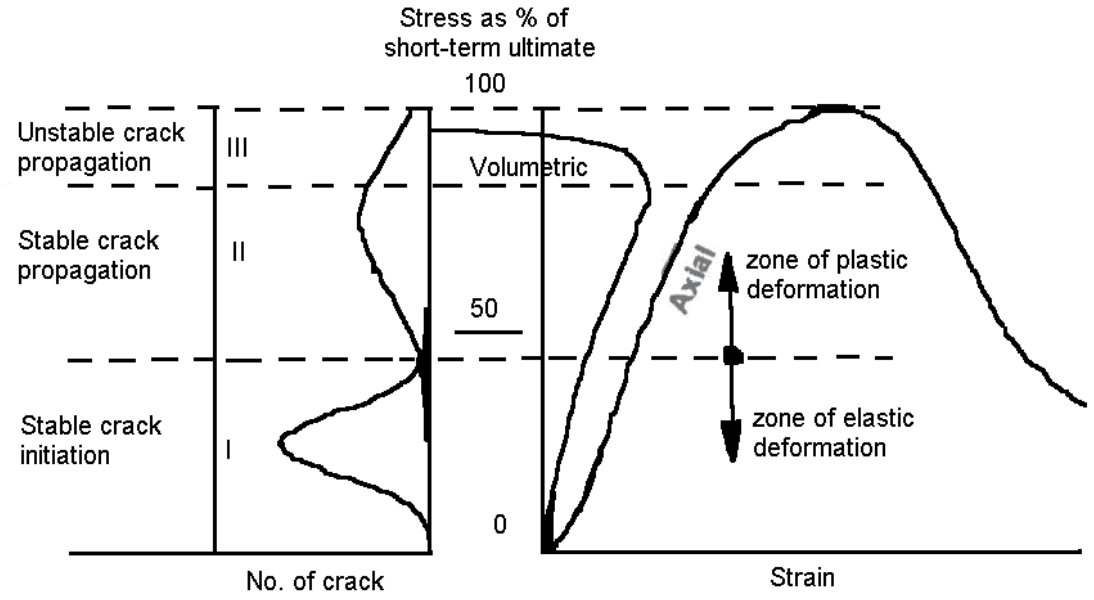

Figure 3.12 Stages of cracking in concrete under compressive load, [Newman(1997a), pg7].

(a) Stage I - Crack initiation

Although some discontinuities exist as a result of the compaction process of fresh concrete, the formation of small fissures or microcracks in concrete is due primarily to the strain and stress concentrations resulting from the incompatibility of the elastic moduli of the aggregate and paste components.Furthermore intrinsic volume changes in concrete due to shrinkage or thermal movements can cause strain concentrations and cracking at the aggregate-paste interface, even before loading

Once loading commences it appears that localised cracks are initiated at the microscopic level at isolated points throughout the specimen where the tensile strain concentration is the largest. Their formation relieves the strain concentration and equilibrium is soon restored, the accompanying energy changes and irrecoverable deformation being small. This shows that these cracks are stable and, at this load stage, do not propagate. Owing to the heterophase nature of concrete, there will be a distribution of strain concentrations throughout the specimen at a given applied load. As the applied load is increased during stage I, there will be a more or less continuous multiplication process of stable crack initiation.

(b) Stage II - Stable crack propagation

During this stage the crack system multiplies and propagates as the applied load is increased, but in a slow stable manner, in the sense that, if loading is stopped and the stress level is maintained at a certain value, crack propagation ceases. Crack initiation (Stage 1) and stable crack propagation (Stage II) clearly overlap and there is a transition phase from one to another which does not occur at any single stress. However, the degree of cracking eventually reaches a more severe level which is easily detectable by acoustic emission, ultrasonic pulse velocity and volume change measurements, and necessarily involves major structural changes.

The extent of the stable crack propagation stage will depend markedly upon the applied state of stress, being very short for ‘brittle’ fractures under predominantly tensile stress

states and longer for more ‘plastic’ fractures under predominantly compressive states of stress.

(c) Stage III - Unstable crack propagation

This occurs when under the particular system of loading, the crack system has developed to such a stage that it becomes unstable and the release of strain energy is sufficient to make the cracks self propagating at constant or even reducing load until complete disruption and failure occurs. ‘Unstable crack propagation’ occurs at about 70 to 90 percent of ultimate stress and is reflected in an overall dilation of the structure. The load stage at which this occurs corresponds approximately to the long term strength of concrete.

Relevance to abrasion resistance

In the context of abrasion in a concrete surface, this stage corresponds to localized crushing, perhaps as a result of stress concentration, as may occur when a loaded forklift with ‘solid’ tyres goes over an aggregate particle. In its smallest denominator, this form of axial crushing is limited to the microscopic protrusions/asperities of the concrete’s surface.

3.3.6.5 Mechanisms of Cracking in Concrete

Concrete is a multiphase material and contains cement paste (unhydrated and hydrated compounds), fluids, aggregates, discontinuities, etc. The overall mechanical and physical properties of such a composite system depend on the volume fractions and properties of the various constituents, as well as upon the mechanisms of interaction, whether mechanical, physical or chemical, between the separate phases.

It follows that in such a system crack propagation paths may occur as follows:

(i) at the aggregate paste interface
(ii) in the cement paste or mortar mix
(iii) in the particles of aggregate

The points of crack initiation will depend upon the relative strength of the cohesive bonds and the local state of stress at these three localities.

Under *uniaxial tensile* states of stress, the fracture path generally runs orthogonal to the maximum tensile stress. For strong natural occurring dense aggregates, the crack path tends to follow the aggregate-paste interface across which the cohesive forces are mostly of the weakly intermolecular van der Waals type. The tensile strength of these concretes is dependent, therefore, mainly on the so-called aggregate-paste tensile bond strength. For tensile states of stress, stable crack propagation (stage II) is of short duration since the cracks propagate very rapidly through the mortar matrix and around the aggregate paste interface. The behaviour is much more unstable under uniaxial tension since cracking tends to reduce the load-carrying area of the specimen. Figure 3.13 indicates that stable crack propagation is indeed short lived, initiating at a microstrain of approximately –70 (- implies tension) with snapping occurring very soon after at a mirostrain of –100. This may be contrasted with the very much greater strains of figure 3.14, for triaxial compression, where the onset of stable crack propagation occurs at 1800 microstrains, failing at 3000 microstrains.

Clearly the axial strain is a function of the tensile stress, (which in turn is a function of the applied load).

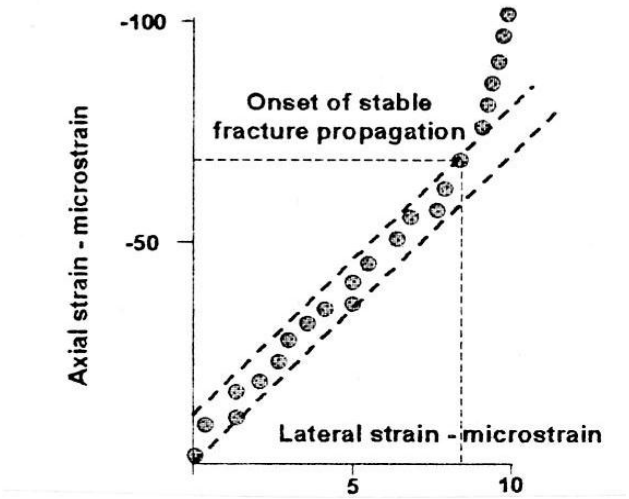

Figure 3.13 Relationship between axial and lateral strains for uniaxial tension, [Newman(1997a), pg 6].

Under *uniaxial compressive* states of stress evidence suggests that, firstly, stable cracks are initiated in the mortar matrix in line with the direction of applied compression. As the load is increased, the cracks multiply and extend in this same direction, until, in the vicinity of mineral aggregate inclusions, the fracture path divides and travels around, rather than through, the hard particles. (This especially applies to coarse aggregate, which has a relatively low paste aggregate surface ratio).The fracture process is more stable than for uniaxial tension since the loaded area is less influenced by the cracking (compare figures 3.13 and 3.14). This translates into a prolonged 'Stage II – Stable Crack Propagation' phase.

In *triaxial compression* (figure 3.14) the three stages are very similar to uniaxial compression, except that stage 2 is more prolonged with increasing lateral stress. Triaxial compression is even of greater interest than uniaxial compression, since in practice, the compression induced lateral strain (according to Poisson's ratio) is substantially contained by the surrounding concrete.

Clearly the lateral restraint (either at asperity level, or in the bulk concrete) will delay the onset of axial cracks, compared to a body in iniaxial compression that is not confined laterally.

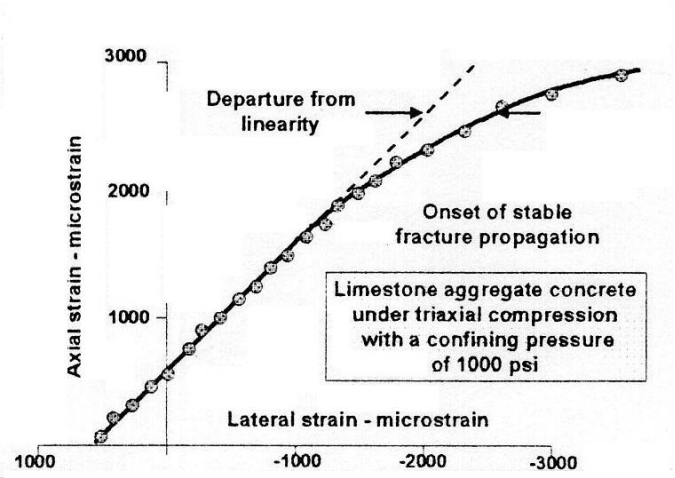

Figure 3.14 Relationship between axial and lateral strains for triaxial compression, [Newman(1997a), pg 6].

3.3.6.6 Relationship between State of Stress and Abrasion Resistance

(a) Uniaxial tension

If compressive strength can be reduced to the rate at which cracks propagate axially, then clearly the uniaxial tensile strength of the concrete will have a bearing on compressive strength. The same may be said of abrasion wear. Severe abrasion, which amounts to macroscopic growth of axial cracks into the core concrete, and mild abrasion which amounts to microscopic axial cracking in the asperities, will clearly also be related to the uniaxial tensile strength.

In the same way the development of cone and lateral cracks will also be related, if not directly proportional, to the uniaxial tensile strength of the concrete.

(b) Uniaxial compression

Uniaxial compression is obviously of interest in a study of abrasion-wear induced by a normal load. This is a common occurance, and typical examples are shown in figure 3.23.

In section 2.1, after considering many investigations, it was concluded that abrasion resistance is positively related to the uniaxial compressive strength, providing no special surface conditons apply.

This is logical since a primary mode of abrasion wear is crushing, either at asperity level, or deeper into the core, and therefore uniaxial compression ought to be a very good indicator of abrasion resistance.

Finally it seems reasonable to propose that whereas a ‘tall’ asperity will fail in uniaxial compression, a ‘squat’ asperity is more like to fail in a state of triaxial compression. In both cases crushing is accompnied by the formation of axial cracks.

(c) Triaxial compression

In concrete that has a substancial lateral dimension, such as a concrete floor, the lateral dilation owing to any vertical stresses, will be greatly restricted by Poisson’s related lateral compression, and logically this limits the development of axial cracks, and therefore increases abrasion resistance. In this respect segmental paving blocks, are unlikely to develop the same degree of lateral compression, as much of the compression will be dissapated by the perimeter filling sand that has a low modus relative to the elastic modulus of the concrete paver.

The principle of a lateral compressive stress developing in response to a vertical stress (which would have the effect of limiting lateral dilation, and hence axial cracking, and hence abrasion resistance) is also demonstrated by Boussinesq’s equasions below.

3.3.6.7 Boussinesq’s Equations

In 1885, Boussinesq supplied equations for determining stresses at a point within an ideal mass. These expressions are given in 3.9 through 3.13 [Cernica(1982)].

The equations are based on the assumption that the mass is an *elastic, isotropic, homogeneous, and semi-infinite medium* which extends infinitely in all directions from a level surface.

Although concrete is not homogenous, nor strictly elastic, Boussinesq’s equations nevertheless provide a basis for illustrating that in a mass of concrete that may be

considered large relative to the area of a normally applied load, confining *lateral* stresses are set up to resist dilation, and this serves to retard the development of axial cracking.

This principle also applies to abrasive loads, which may be considered either as highly concentrated *point loads* on the one hand, or alternatively as *uniformly distributed loads*. Both these possibilities will be considered.

(a) Boussinesq's equations for a point load

Surfaces are for example subjected to point loads when a grain of sand is pressed into the surface, typically by a vehicle or pedestrian.

Expressions 3.9 through 3.11 show that both the vertical stress ρ_z and the horizontal stresses ρ_y,and ρ_x acting on a given element are directly proportional to the point load W. The magnitude of these stresses are clearly also very sensitive to the location of the element relative to the point load, as indicated by the distances z, x, y, R in the equations. The symbols z, x, y, W, R, σ_x, σ_y, σ_z are also illustrated in figure 3.15 (a)

$$\sigma_z = \frac{3Wz^3}{2R^5} \quad \text{..... (3-9)}$$

$$\sigma_x = \frac{3W}{2\pi}\left\{\frac{x^2 z}{R^5} + \frac{1-2\nu}{3}\left[\frac{1}{R(R+z)} - \frac{(2R+z)x^2}{R^3(R+z)^2} - \frac{z}{R^3}\right]\right\} \quad \text{..... (3-10)}$$

$$\sigma_y = \frac{3W}{2\pi}\left\{\frac{y^2 z}{R^5} + \frac{1-2\nu}{3}\left[\frac{1}{R(R+z)} - \frac{(2R+z)y^2}{R^3(R+z)^2} - \frac{z}{R^3}\right]\right\} \quad \text{..... (3-11)}$$

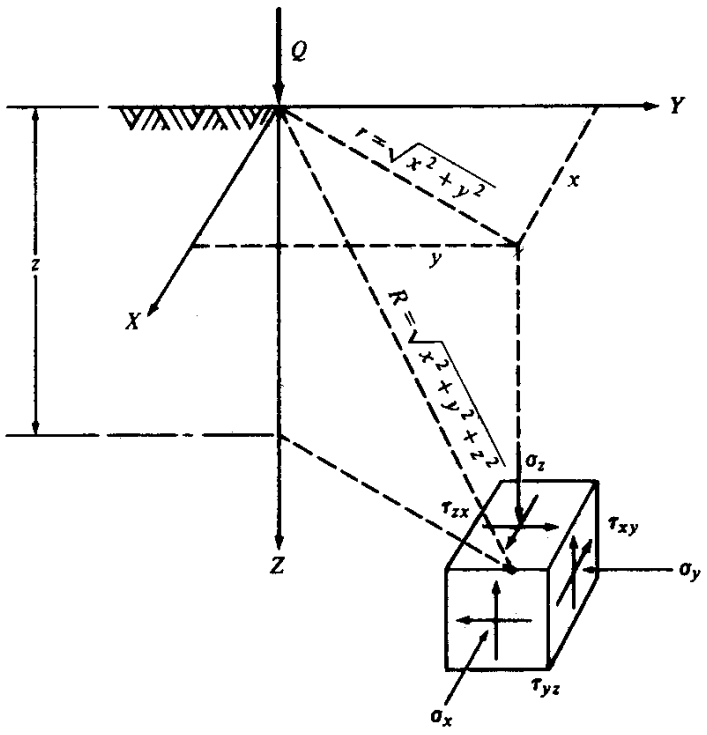

Figure 3.15 (a) Stresses on an element subjected to a concentrated load W, (rectangular coordinate notation). [Cernica(1982), pg161].

The convention indicated in the diagram shows that stresses causing the element to be compressed are possitive, and therefore negative for vice versa (in a given direction).

Finally, as Poisson's ratio, μ increases, so do the lateral stesses. This makes sense qualitatively but is not readily discernable from expressions 3.10 and 3.11.

To illustrate the sensitivity of equations 3.9 through 3.11 to the relative location of the element from the point load, differing values have been assigned to x, y, and z in table 3.1, while W and ν have been treated as constants, assumed to be 1 and 0,22 respectively.

Table 3.1 Boussinesq's Equations as Applied to a Point Load

z	x	y	W	R	ν	σ_z	σ_x	σ_y	$\%\sigma_x/\sigma_z$
mm	mm	mm	N	mm		N/mm^2	N/mm^2	N/mm^2	
0.01	0	0	1	0.01	0.22	4772.727	-445.455	-445.455	-9
0.1	0	0	1	0.1	0.22	47.72727	-4.45455	-4.45455	-9
1	0	0	1	1	0.22	0.477273	-0.04455	-0.04455	-9
10	0	0	1	10	0.22	0.004773	-0.00045	-0.00045	-9
100	0	0	1	100	0.22	4.77E-05	-4.5E-06	-4.5E-06	-9
0.01	0.01	0.01	1	0.02	0.22	306.1706	220.4428	220.4428	72
0.1	0.1	0.1	1	0.17	0.22	3.061706	2.204428	2.204428	72
1	1	1	1	1.73	0.22	0.030617	0.022044	0.022044	72
10	10	10	1	17.32	0.22	0.000306	0.00022	0.00022	72
100	100	100	1	173.21	0.22	3.06E-06	2.2E-06	2.2E-06	72
0.01	0.02	0.02	1	0.03	0.22	19.64085	62.0651	62.0651	316
0.1	0.2	0.2	1	0.3	0.22	0.196409	0.620651	0.620651	316
1	2	2	1	3	0.22	0.001964	0.006207	0.006207	316
10	20	20	1	30	0.22	1.96E-05	6.21E-05	6.21E-05	316
100	200	200	1	300	0.22	1.96E-07	6.21E-07	6.21E-07	316

The following may be concluded from Table 3.1 and expressions 3.9 through 3.11.

(i) Considering the case of x and y =0, σ_z rapidly diminishes with increasing depth, z. From expression 3.9 it is evident that σ_z is effectively proportional to the inverse of the square of the depth, and directly proportional to the applied load,.W. At shallow depths these stresses can be very substantial, even with a nominal point load of 1 N. (The word 'nominal' is perhaps misleading, since in practice the microscopic asperities, which are each assumed to carry 1 N (in this illustration), may be very concentrated. Thus if there are 10 asperities in a mm^2, then this clearly translates into an average nominal stress of 10 MPa.

(ii) Still considering the case of x and y = 0, σ_y and σ_x are seen to be negative. This implies that there is a vertical line immediately beneath the point load that is in tension. This is confirmed by figure 3.9, which shows a vertical 'pin' like crack immediately beneath the point load. However, these tensile stresses while very intense at the surface soon dissipate with increasing depth and are seen to be very small by a depth of 1mm. It appears from table 3.1 that σ_x is approxiamately 1/10th of σ_z,regardless of depth, and since concrete is generally considered to have a tensile stress approximately 1/10th that of the compressive strength, it is likely the surface at these very shallow depths will fail in compression and tension simultaneously.

(iii) Conrarywise to (b) above, the lateral stresses acting on elements away from the axis of the point load are possitive in both the x and y directions, and soon

become greater than the vertical stess as indicated by the ratio $\%\sigma_x/\sigma_z$, which is greater that 100% by the time x and y are 0,02 mm Thus although σ_y and σ_x decrease with increasing distance from the axis of the point load, the ratio σ_x/σ_z rapidly increases.

Sectional summary and conclusion

It may be concluded that the application of a point load to a concrete surface results in *lateral compression*, and this *will inhibit the development of axial cracks*, other than a 'pin' crack along the axis of the point load.

Even small forces, when acting as a point load, have the ability of cracking the concrete, albeit to a very shallow depth The cumulative effect of this no doubt plays a role in the gradual attrition of the surface under such conditions.

On the other hand, it is also apparent that a distributed load that only makes contact with the tips of microscopic asperities may be regarded as a point load, as far as each affected asperity is concerned, with abrasive effects.

Finally, it may be said, that whereas Boussinesq'a equasions are usually applied to determine stresses in soils, where the zone of investigation often covers a few meters, by using these formuli on a microscopic/millimeter scale it is possible to explain the development of very high tensile stresses very close to the surface, thus accounting for gradual wear with time. Again, using Boussinesq's equasions for concrete rather than soils is justified on the basis that concrete likely better satisfies his initial assumptions, particularly as regards elasticity and isotropicity.

(b) Boussinesq's equations for a uniformly distributed load

In practice, however, true *point* loads are seldom encountered, unless veiwing the surface microscopically, as considered above. In this case every asperity is potentially the site of a point load. This is not unrealistic, given that true contact between two surfaces will inevitably be at their topmost asperities and the corresponding areas of contact may therefore be very small indeed.

On the other hand, taking more of a macroscopic view, even a grain of sand has a finite bearing area, and may therefore, be considered as applying a *distributed* load.

The simplest case of a distributed load is a uniformly distributed load, such as when a vehicle traverses a clean and smooth surface. (Clearly the corresponding pressure in this case is far less than that occurring under a grain-of-sand)

Boussinesq's equation [see expression (3-9)] can be applied to determine the unit vertical stress on a uniformly loaded *circular* area at any given depth [see figure 15.3(b)]. Thus expression (3-12) defines the vertical stress, $\sigma_{z,}$ acting along a central axis and at a depth z below the applied uniformly distributed load, q. Note that q is obtained by dividing the total load by its footing area, i.e. $q = Q/\pi r^2$).

$$\sigma_z = \frac{3qz^3}{2\pi}\int_0^{2\pi}\int_0^{r}\frac{\rho\cdot d\beta d\rho}{\left(\rho^2+z^2\right)^{5/2}} \quad \ldots\ldots\ (3\text{-}12)$$

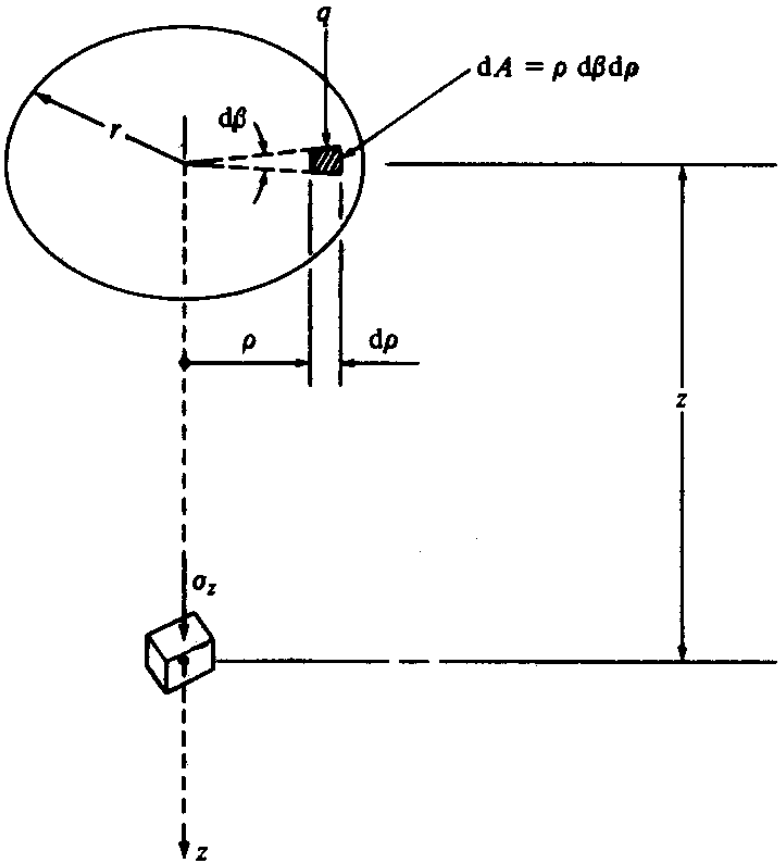

Figure 3.15 (b) Vertical stress under centre of loaded circular area [Cernica(1982), pg176].

Expression 3.12 may be simplified as:

$$\sigma_z = q\left[1-\frac{1}{\left(r^2/z^2+1\right)^{3/2}}\right] \quad \ldots\ldots \text{3-13}$$

No formula is given for σ_y and σ_x, but given the lateral restraint within a large body of material these values may be assumed to be equal to the product of Poisson's ratio and the applied stress, i.e.:

$$\sigma_y = \sigma_x = \sigma_z \cdot \nu \quad \ldots\ldots\ (3\text{-}14)$$

Note that the lateral pressure at the surface is $\nu \cdot q$ (substituting 0 for z in exp 3-13 and q for σ_z in exp 3-14).

Thus $\sigma_y = \sigma_x = \sigma_z \cdot \nu$ ..... (3-14a)

Using Poison's ratio in expression (3-14a) may be justified as follows: To satisfy vertical equilibrium, the vertical stress at the surface will be the same as the applied normal stress. This element will strain in a vertical direction, and in so doing attempt to dilate in a lateral direction, the magnitude of the dilation being governed by Poisson's ratio. However, in the

case of a uniformly distributed load covering a relatively large area, any lateral strain is prevented by adjacent elements attempting to strain at the same rate but in opposing direction. The extent that the lateral strain is prevented translates into a lateral stress, the magnitude being related to the vertical applied stress by Poison's ratio. Thus for example, a vertical stress of 10MPa would in these circumstances result in a not insignificant lateral stress of 2,2 MPa, if Poisons ratio is 0,22.

As in the case of point loads this lateral compression serves to inhibit axial cracking and thereby abrasion wear. But unlike a point load no 'pin' cracking accompanies the process, as the whole area below the footing is in a state of lateral compression.

3.3.6.8 Sectional Summary and conclusion

Section 3.3.6 may be concluded by stating that the vertical compressive stresses associated with abrasive loads may result in 'axial' cracks developing that propagate in the direction of the maximum principal compressive stress. In this process the concrete dilates laterally. However concrete floors, as opposed to concrete test cylinders, are substantially constrained in the lateral direction. Therefore the imposition of a vertical stress on a body of concrete that has minimal scope for lateral strain, particularly where the load is distributed over an appreciable area, results in lateral compressive stresses being set up that substantially restrain 'axial' cracks (and thus also abrasion).

Having said this cracking may still occur in certain situations, and this will clearly be a function of the magnitude of the vertical applied stress and consequent axial and lateral strains. Accordingly it may be said that:

- A sufficiently large vertical stress will induce axial cracking regardless of lateral confinement.
- The onset of axial cracks occurs at a higher stress where there is full lateral confinement relative to no confinement.
- Point loads may be so concentrated that the vertical stress is extremely high, resulting in surface crushing/cracking at *very* shallow depths e.g.0.01mm, but by 0,1mm the stress is substantially dissipated.

In the case of 'mild' abrasion these cracks will be substantially restricted to the surface asperities, leading to slight wear, whereas with 'severe' abrasion, cracks may penetrate into the 'core' zone, and the rate of abrasion wear will be much greater.

Recommendation: Further research into the extent that lateral compression limits abrasion resistance by reducing axial cracking in concrete slabs is recommended.

3.3.7 Hard Particle Effect

Figure 3.3 (g) indicates a hard particle trapped between a load and the concrete surface. This has the potential of greatly increasing the stress, leading to any of the forms of cracking described in 3.3.4 through 3.3.6. On the other hand the stress intensity may be less, depending on the load and the contact area of the hard particle, resulting in either elastic or plastic deformation. Some adhesion is also possible. It may therefore be said that hard particles between load and counterface may result in any of the surface contacts described in figure 3.3.

Hard particle effect is probably the most important of all in terms of abrasion wear on concrete surfaces. Without this effect abrasion would mostly be limited to the effects of relatively soft footwear and tyres, resulting in elastic deformation mostly, and wear would be virtually nil.

Hard particles may be introduced to the surface in a number of ways; from construction vehicles losing coarse or fine aggregate leaking from their tail gates; from aggregate that is loosened out of an existing surface; wind blown sand and dust, surely the most common source.

Large hard particles have the ability to lift the load, and consequently take on a greater percentage of the load, relative to small particles. In contrast a few sand particles beneath a rubber tyre do not have the effect of raising the level of the axle, the flexible rubber merely covering the particle. Large particles are therefore more severe stress concentrators.

Although sand particles do not generally raise the level of the axle, they still have the potential to apply a considerable stress to the surface. The rubber in effect domes over the sand particle, and in stretching results in a tensile force that has a downward vertical component that forces the particle into the surface. This is in addition to the normal pressure of the tyre on the particle. This effect is illustrated in figure 3.16.

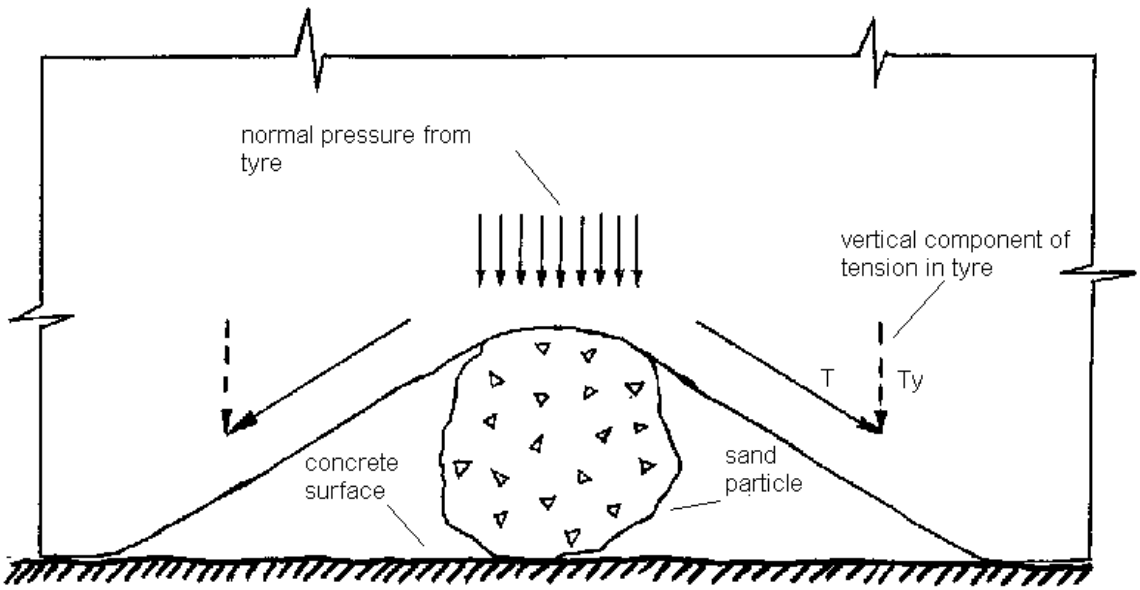

Figure 3.16 Tension dome effect, where a rubber tyre covers a sand particle. This has the effect of magnifying the compression between sand and surface.

The severity of the tension dome effect is clearly dependant on the degree of stretch in the tyre at that locality, and hence the smaller the particle the lower is this abrasive effect.

Aggregate particles are most abrasive when they make contact with an element of cement paste, since most aggregate is substantially harder than paste (i.e. > 1,2 times as hard). On the other hand a piece of dust which comes to rest on a protruding/exposed *aggregate* particle, which is as hard or possibly even harder than the abrasive (dust particle), will at worst result in very slight polishing when pressed down by traffic.

Clearly abrasive particles that are angular in shape with sharp corners will be more destructive. Hutchings(1992) showed that sharp angular particles were ten times more abrasive than rounded particles. Clearly sharp particles have the ability of cutting by means of greatly intensifying the compressive/tensile stress effects at the leading edge (leading to plastic deformation and cracking effects). Their irregular shapes also allow them to probe between aggregate particles, attacking the relatively weak paste matrix in these areas, thereby leading to earlier plucking out to the surface aggregate.

In summary it may be said that hard particles under load lead to both deformation and cracking of the surface. They are virtually omnipresent on surfaces, appear in various shapes and sizes, and contribute very significantly to abrasion wear.

3.3.8 Sectional Summary

In this section (section 3.3) the abrasive effects of adhesion, elastic and plastic deformation, and three possible modes of cracking were considered under conditions of direct compression.

Hard particles act as considerable ‘stress multipliers’, and are generable responsible for the bulk of crushing related abrasion wear.

In the next section the additional effect of lateral movement is considered.